

Published in final edited form as:

Int J Radiat Oncol Biol Phys. 2025 April 01; 121(5): 1372–1383. doi:10.1016/j.ijrobp.2024.11.092.

Characterization of a time-resolved, real-time scintillation dosimetry system for ultra-high dose rate radiation therapy applications

Alexander Baikalov, MS^{1,2,3}, Daline Tho, PhD¹, Kevin Liu, MS^{1,4}, Stefan Bartzsch, PhD^{2,3}, Sam Beddar, PhD^{1,4,*}, Emil Schüler, PhD^{1,4,*}

¹Department of Radiation Physics, The University of Texas MD Anderson Cancer Center, Houston, TX, United States

²Department of Radiation Oncology, School of Medicine and Klinikum rechts der Isar, Technical University of Munich, Munich, Germany

³Institute of Radiation Medicine, Helmholtz Zentrum München GmbH, German Research Center for Environmental Health, Neuherberg, Germany

⁴The University of Texas MD Anderson Cancer Center UTHealth Graduate School of Biomedical Sciences, Houston, TX, United States

Abstract

Background: Scintillation dosimetry has promising qualities for ultra-high dose rate (UHDR) radiotherapy (RT), but no system has shown compatibility with mean dose rates (\overline{DR}) above 100 Gy/s and doses per pulse (D_p) exceeding 1.5 Gy typical of UHDR (FLASH)-RT. The aim of this study was to characterize a novel scintillation dosimetry system with the potential of accommodating UHDRs.

Methods and Materials: We undertook a thorough dosimetric characterization of the system on an UHDR electron beamline. The system's response as a function of dose, \overline{DR} , D_p , and the pulse dose rate (DR_p) was investigated, as was the system's dose sensitivity (signal per unit dose) as a function of dose history. The capabilities of the system for time-resolved dosimetric readout were also evaluated.

Results: Within a tolerance of $\pm 3\%$, the system exhibited dose linearity and was independent of \overline{DR} and D_p within the tested ranges of 1.8–1341 Gy/s and 0.005–7.68 Gy, respectively. A 6% reduction in the signal per unit dose was observed as DR_p was increased from 8.9e4 to 1.8e6 Gy/s. The dose delivered per integration window of the continuously sampling photodetector had to remain between 0.028 and 11.56 Gy to preserve a stable signal response per unit dose. The system accurately measured D_p of individual pulses delivered at up to 120 Hz. The day-to-day variation of the signal per unit dose in a reference setup varied by up to $\pm 13\%$ but remained consistent ($<\pm 2\%$) within each treatment day and showed no signal loss as a function of dose history.

^{*}Correspondence: to Sam Beddar: abeddar@mdanderson.org and Emil Schüler: eschueler@mdanderson.org. Conflicts of Interest: None.

Conclusions: With daily calibrations and DR_p -specific correction factors, the system reliably provides real-time, millisecond-resolved dosimetric measurements of pulsed conventional and UHDR beams from typical electron linacs, marking an important advancement in UHDR dosimetry and offering diverse applications to FLASH-RT and related fields.

Introduction

Precise and reliable dosimetry is a fundamental component of safe and successful radiation therapy (RT). Recent advances in ultra-high dose rate (UHDR, higher than ~40 Gy/s) FLASH-RT protocols, in contrast with conventional dose rate (CDR, ~0.1Gy/s) RT, present unique challenges to dosimetry. Saturation effects due to the high particle fluxes present at UHDRs render most conventional radiation detectors unreliable, necessitating the development of specially designed UHDR detectors (1).

The essential characteristics of traditional detectors for CDR-RT, including real-time signal readout, high accuracy and precision, a linear response to dose, and independence from beam quality and dose rate, continue to be crucial for UHDR detectors. However, UHDR detectors face significantly greater demands, particularly for high-energy electron and photon deliveries, where conventional detectors and dosimeters display signal saturation and dose rate–dependent readouts (1-3). These deliveries, using UHDR-capable linear accelerators, often consist of just one or a few microsecond-long pulses at up to 360 Hz, with doses per pulse (D_p) up to ~10 Gy, pulse dose rates (D_p) on the order of MGy/s, and mean dose rates (D_p) on the order of kGy/s (4). UHDR detectors must therefore be dose rate—independent over an extreme range of dose rates and exhibit dose linearity across a large range of nearly instantaneously delivered doses. Ideally, a UHDR detector should also have a high enough temporal resolution to differentiate between pulses, with a goal of sub-microsecond resolution to measure parameters like pulse width (PW) (5).

Scintillation dosimetry has been studied extensively in various CDR-RT contexts, and scintillator detectors have many characteristics that are ideally suited for FLASH-RT applications (6). Organic plastic scintillators have a very fast response time (<15 ns) with a linear dose response, are water equivalent at relevant energies, are dose rate-independent (at CDRs), and can be made very small whilst retaining sensitivity (7-10). Plastic scintillators operate on the following principle: radiation-induced electronic excitation of the scintillating material results in photon emission after deexcitation (within nanoseconds) directly proportional to the absorbed dose. An optical fiber is typically used to guide this scintillation signal to a detector. However, Cherenkov and fluorescence radiation from within both the scintillator and the fiber contaminate the scintillation signal and must be dealt with appropriately as they are not dose-proportional; many methods for this have been developed (9,11,12). Quenching effects due to partially non-radiative relaxation after high linear energy transfer (LET) radiation must also be considered (13,14). However, dosimetry in UHDR proton beams does not face the same limitations as encountered in electron and photon beams due to their lower instantaneous dose rates. Therefore, standard clinical dosimetry solutions such as ion chamber dosimetry can be directly employed with maintained high dosimetric accuracy as seen in CDR clinical dosimetry (1,15,16).

Plastic scintillators thus seem to be good candidates for low-LET UHDR beamlines, although limited research into their responses at UHDRs exists. One plastic scintillator was studied under x-ray radiation, indicating good performance up to the highest tested dose rate of 118.0 Gy/s (17). A 2D plastic scintillation detector(18) and three point detectors(19-21) were studied under UHDR electron radiation, also indicating good performance at the lower end ($D_p < 1.5 < 1.5$ Gy and $\overline{DR} < 380 < 380$ Gy/s) of UHDR parameter ranges. However, radiation damage was noted(20,21) and, at more extreme values of D_p , \overline{DR} , and the pulse repetition frequency (PRF), nonlinear responses and signal saturation were observed (21).

In this work, we performed a detailed characterization of a novel FLASH-dedicated scintillation dosimetry system and tested its capabilities in providing real-time, highly time-resolved dosimetric data. The system provides a high sample rate of up to 1 kHz, thereby resolving individual pulses from typical linear accelerators, and includes a high dynamic range to handle the high doses per pulse of FLASH-RT. We demonstrated its dose linearity and pulse-by-pulse dose measurement capabilities in a comprehensive evaluation on a flexible UHDR electron beamline up to the highest tested values of PRF 120 Hz, \overline{DR} 1340 Gy/s, and D_p 7.7 Gy.

Methods and Materials

Scintillation Dosimetry System

The prototype Hyperscint RP-FLASH scintillation dosimetry system (MedScint, Quebec City, Canada) comprises a plastic scintillator probe with a cylindrical active volume of 1 mm diameter x 3 mm length connected via a polymethyl methacrylate plastic optical fiber to a spectrometer with a cooled 2D photodetector array. During measurement, the photodetector collects the light spectrum from the probe over a set 'integration window' (IW) after which an automatic signal readout process is performed. The integration window determines the sampling frequency ($f_s = 1 / W$) of the measurement. If IW>40 ms (f_s <25 Hz), the system operates in 'continuous mode', whereby it continues to record at the set sampling frequency until the measurement is stopped by the user. Otherwise, if IW<40 ms, the system operates in 'FLASH mode', where a fixed number of IWs (samples) are recorded, with a maximum sampling frequency of 1000 Hz. The recorded spectrum per IW is automatically processed by the vendor-supplied HyperDose software using a hyperspectral approach to isolate the scintillation, fluorescence, and Cherenkov signals (22).

This hyperspectral approach requires a spectral calibration, done according to the vendor-specified protocol, involving irradiation of the probe and fiber with both kV and MV beams. A dosimetric calibration can also be done to relate the signal output of the system to a known dose. The vendor provided both a spectral and a dosimetric calibration, both done before we received the device. After obtaining all of the measurements specified in this work, we performed our own spectral and dosimetric calibrations on a clinical linear accelerator calibrated according to AAPM protocol TG-51 (23). By retrospectively applying either the vendor-provided or the self-performed calibration files to the measured data, the influence of either on the results could be directly compared. We report the system's signal

intensity in arbitrary units throughout this work. The scintillator and spectrometer were never decoupled.

Measurement Setup

Irradiation measurements were performed with a 9 MeV electron beam from an electron linear accelerator (Mobetron, IntraOp, Sunnyvale, CA, USA) capable of both CDR and UHDR radiation delivery (24,25). For all measurements, the probe was placed between two 1-cm sheets of water-equivalent, flexible bolus material, with the active region of the probe centered in the radiation field (Figure 1). At least 7 cm of backscatter solid water material was placed underneath the bolus sheets.

The UHDR beam parameters directly adjustable on the Mobetron were as follows: number of pulses (N_p) , source-to-surface distance (SSD) from 25.8–111.2 cm, pulse repetition frequency (PRF) from 5–120 Hz, and pulse width (PW), measured by the full-width at half-maximum) from 0.5–4 μ s. These parameters affected the following dose-related parameters: total dose (D), dose per pulse $(D_p = D / N_p)$, pulse dose rate $(DR_p = D_p / PW)$, mean dose rate $(\overline{DR} = D / (((N_p - 1) / PRF) + PW)))$, and dose per integration window of the photodetector $(D_{lw} = D / IW)$. The following CDR beam parameters were held constant: $PW = 1.2 = 1.2 \,\mu$ s and $PRF = 30 \,\mu$ Hz. In both CDR and UHDR modes, the output beam current of the Mobetron was not adjustable; thus, DR_p could be varied only by varying the SSD.

Before each measurement session, the spectrometer was powered on for a few minutes until it reached a stable temperature, which was indicated by the system's software. Unless otherwise specified, each UHDR measurement consisted of the delivery of 3 pulses at 30 Hz, whereby the average signal per pulse was recorded. Each 3-pulse measurement was performed in triplicate, the average of which is reported with an error bar representing one standard deviation. Some graphs contain error bars that are smaller than the symbols used to represent the values and thus are not visible. IW was set to 4.1 ms ($f_s = 244$ Hz) to exceed the Nyquist frequency of the highest possible beam delivery PRF of 120 Hz, and the number of samples per measurement was set to 800, resulting in a measurement length of 3.28 s. The start of each measurement was manually timed to coincide with the delivery of the beam, and the correct relative timing of the measurement start to the beam delivery was verified by ensuring that the number of pulses recorded on the system matched the number of pulses recorded by external beam-current transformers (BCTs, Bergoz Instrumentation, Saint-Genis-Pouilly, France) used to monitor the beam.

To determine the dose delivered to the probe for each measurement, dose was measured by using dose rate—independent radiochromic film (Gafchromic EBT3, Ashland Inc., Covington, KY, USA) for each unique combination of *SSD* and *PW* used in this work. The film was placed at the location of the probe, between the two sheets of bolus, and the statistical errors across triplicate film dose measurements were propagated to the final reported values. Dose readout of the film was achieved by using a previously described protocol (26). Simultaneously, a beam monitoring detector (either a BCT or an ionization chamber, depending on the irradiation dose rate) was used to monitor the

beam output. Subsequent irradiations of the probe did not include film but instead relied on the relative output of the beam monitoring detector, calibrated to the film dose at the probe location of each setup, thereby accounting for any variations in the beam output. For CDR measurements, the dose was determined as described above, but was monitored by using an Advanced Markus ionization chamber (PTW-Freiburg GmbH, Freiburg, Germany) placed at a set location below the probe (embedded in the solid water [Figure 1]). For UHDR measurements, inline BCTs were used as previously described (27,28). The BCTs yield highly-time-resolved measurements of the beam current for each individual pulse delivered and were used as the reference against which the scintillator system's response was compared. To compute the BCT signal per pulse, each BCT signal was integrated over a region corresponding to 160% of the full-width at half maximum of the pulse.

System Dose Response and Stability at CDRs

All CDR measurements were obtained using the same reference setup (Figure 1) under an uncollimated field at a fixed source-to-surface distance (*SSD*) of 35.8 cm, varying only the parameters D, IW, and therefore D_{iw} . First, the system's response as a function of D_{iw} was evaluated from 0.007–13.94 Gy by adjusting D and IW (the specific parameters are shown in Table 1, **experiment I**). Second, the system's response as a function of D was evaluated from 0.05–17.2 Gy at fixed values of IW = 1 s. D_{iw} therefore ranged from 0.05–0.14 Gy (Table 1 **experiment II**). Finally, the stability of the system over 10 non-consecutive days and ~3 kGy of accumulated dose was evaluated by periodically measuring a triplicate delivery of 2.42 ± 0.04 Gy with IW = 1 s (thus, $D_{iw} = 0.14$) (Table 1 **experiment III**).

System Dependency on $D_{\scriptscriptstyle p}$

To study the system's response at UHDRs as a function of D_p , the D_p was varied by (1) changing the PW while keeping the DR_p constant (Figure 2a) (Table 1 **experiment IV**), or by (2) changing DR_p while keeping the PW constant (Figure 2b) (Table 1 **experiment V**). In condition 1, the probe was exposed to pulses of varying PW (0.5–4 μ s) at a constant DR_p . This was repeated for two different DR_p , the highest and lowest possible with the experimental setup, to achieve a wider range of D_p . In condition 2, to study the system's linearity with D_p at a constant PW but varying DR_p , the probe was irradiated at varying SSD. Because the field was uncollimated, the amount of exposed optical fiber increased with the SSD.

System Dependency on \overline{DR} , PW, and DR_p

To determine if the system's response was influenced by \overline{DR} , the PRF was varied while keeping all other parameters constant (Figure 2c) (Table 1 **experiment VI**). The PRF was varied between 5–120 Hz, resulting in a total time between two sequential pulses of 8.3–200 ms. These measurements were repeated at two different SSDs, and thus two different DR_p , the highest and lowest possible with the experimental setup, to cover a wider range of \overline{DR}_p . To determine the system's response when varying both PW and DR_p at a constant D_p , the probe was exposed to a constant D_p by increasing the PW as the SSD was increased (Figure

2d) (Table 1 **experiment VII**). These measurements were repeated for two different values of D_{o} : 4.01 ± 0.12 Gy and 1.00 ± 0.02 Gy.

Pulse Discrimination and Pulse-by-pulse $oldsymbol{D}_p$ Measurement

To study the system's ability to differentiate between pulses and reliably measure D_p of individual pulses, 300 pulses were delivered at 30 Hz and $D_p = 0.1$ Gy (Table 1 **experiment VIII**). The system's response was recorded and compared with the beam current recorded by the BCTs for each individual pulse. This was performed at three different values of IW to vary f_s : equal to the Nyquist frequency, slightly greater than the Nyquist frequency as recommended by the vendor, and at approximately double that frequency.

Results

System Dose Response and Stability at CDRs

The signal per unit dose varied by less than $\pm 2\%$ for D_{lw} within 0.028-11.56 Gy but was lower when $D_{lw} < 0.007$ Gy or $D_{lw} > 12.5$ Gy (Figure 3a). Choosing a D_{lw} of 0.05-0.14 Gy, the signal increased linearly with D across the entire tested range; the dose-normalized signal varied by less than $\pm 3\%$ (Figure 3b). Periodic measurements over the course of 10 non-consecutive days revealed a general variance of the signal by up to $\pm 13\%$, during which the probe was exposed to ~ 3 kGy of accumulated dose (Figure 3c). A variation of less than $\pm 2\%$ was observed within each day. No signal degradation as a function of either time or dose was evident. Immediately subsequent measurements within each triplicate varied on average by $0.2 \pm 0.2\%$.

System Dependency on D_p

The dose-normalized signal varied by less than $\pm 3\%$ as D_p was changed from 0.04–0.35 Gy and from 0.95–7.28 Gy at two constant SSDs by varying the PW (Figure 4a-b). A ~6% decrease in the signal response per unit dose was observed as D_p was increased from 0.36–7.68 Gy at a constant PW by varying the SSD (Figure 4c).. This trend persisted even after a recalibration of the system and after collimation of the field to equalize the amount of exposed optical fiber at each SSD.

System Dependency on \overline{DR} , PW, and DR_n

The signal varied by less than $\pm 1\%$ with changes in \overline{DR} at both tested DR_p values (8.6e4 Gy/s and 1.9e6 Gy/s) (Figure 5a). The signal per unit dose was unaffected by varying PW and SSD at a constant D_p at both tested values of D_p (Figure 5b). Although the values varied by $\pm 3\%$, no general trend was apparent, and the variance was comparable in magnitude to the uncertainty of each measurement.

Pulse Discrimination and Pulse-by-pulse D_{ν} Measurement

The D_p recorded by the system agreed with the BCTs within $\pm 2\%$ except for occasional notable outliers, where the system recorded a $D_p \sim 2-6\%$ lower than the BCTs (Figure 6a). These outliers were due to the 'split pulse' phenomenon, whereby the signal from one

pulse is split, albeit largely unequally, between two adjacent integration windows of the detector (Figure 6b). The assumed timing of the electron pulses relative to the system's integration windows that could have caused the observed split pulses is overlaid on Figure 6b. This effect can be corrected for (see Discussion for details). In all, 13% of pulses needed a correction of 1–5%, and no pulses needed a correction of >5%. The magnitude and frequency of these split pulses are apparent in Figure 6a, where the raw scintillator signal is low.

For the corrected pulses, as long as the sampling frequency remained higher than the Nyquist frequency (2*PRF), individual pulses were reliably measured without any aliasing. Sampling at exactly the Nyquist frequency did occasionally lead to aliasing, which suggests that the true sampling frequency of the system may be slightly lower than that set by the user. Sampling at double the Nyquist frequency did not reduce the occurrence rate of 'split pulses'. The average recorded PRF from the system matched that of the BCTs. No differences were observed between the lower and higher tested D_p and PRF values.

Discussion

Plastic scintillators like the one studied in this work are appropriate candidates for low-LET UHDR beamlines, although research into their responses at UHDRs is limited. Cecchi et al.(17) used the Hyperscint RP100 (MedScint, Quebec City, Canada) on an UHDR x-ray tube, demonstrating \overline{DR} linearity from 3–118 Gy/s. Favaudon et al.(18) used the 2-D LynxTM detector (FIMEL, Fontenay-aux-Roses, France), demonstrating dose linearity at DR, from 0.4-3.5 MGy/s and D_n up to 3.5 Gy, but noted that the CCD camera used to detect the scintillating light had a limited dynamic range. Poirier et al. investigated the Hyperscint RP100 on an UHDR electron beamline, demonstrating dose linearity with D₀ from 0.2– 0.55 Gy (DR_p = 0.04-0.11 MGy/s) and pulse counting measurements at 2.5 ms resolution. However, these pulse counting measurements suffered from a phenomenon they refer to as 'double peaks', which lead to erroneously low D_{ρ} measurement in a small percentage of pulses (19). Ashraf et al.(20) investigated the Exradin W1 (Standard Imaging, Middleton, WI), demonstrating \overline{DR} independence from 50–380 Gy/s and dose linearity with D_{ϱ} from 0.1–1.3 Gy/s (DR_p =0.1–3.5 MGy/s) but noting significant radiation damage: 16% sensitivity loss per kGy. No temporally resolved measurements were reported in this investigation. Finally, Liu et al.(21) characterized the Exradin W2 (Standard Imaging), demonstrating PW dependencies and radiation damage but otherwise good performance at $D_p < 1.5$ Gy and PRF <90 Hz, but measured a nonlinear response and signal saturation at $D_p > 1.5$ Gy and PRF>90 Hz. The commercially available Hyperscint RP100 and Hyperscint RP200 have been previously characterized at CDRs, exhibiting excellent dosimetric responses (29-32).

In this work, we expand on previous studies by testing higher ranges of UHDR parameters relevant to FLASH-RT of the Hyperscint RP-FLASH scintillation dosimetry system. In line with previous publications(19), and in the absence of a formal standard established for FLASH detectors, we consider a signal variance of up to $\pm 3\%$ from its expected behavior to be an acceptable tolerance standard.

At CDRs, an apparent limitation of the system is that D_{iw} must remain within a given range, 0.028–11.56 Gy, to yield a stable signal per unit dose. Given a D_{iw} value within that range, the system demonstrates excellent signal linearity with dose. The D_{iw} limitation manifests as a limitation on the temporal resolution of low-dose-rate measurements. For example, at \overline{DR} = 0.1 Gy/s, IW must be >0.28 s to ensure D_{iw} >0.028 Gy. Similarly, as discussed below, the upper limit of D_{iw} limits the maximum measurable \overline{DR} and/or D_{g} .

The consequences of the D_{iw} limitations manifest at UHDRs as limitations of the maximum measurable \overline{DR} and/or D_p . Keeping D_{iw} at <11.56 Gy with the system's highest possible time resolution of IW=1 ms limits the \overline{DR} to <11,560 Gy/s. On the other hand, the highest measurable D_p is 11.56 Gy. These limitations are of little concern to clinical applications as few machines are capable of delivering such high \overline{DR} and D_p , and the system's operable range covers the clinically relevant parameter space (33-35).

The D_{iw} value limitation is likely caused by limitations in the dynamic range of the photodetector, similar to the limitation in the CCD of the Lynx system noted by Favaudon et al. (18). Because the saturation occurs not in the scintillating material of the probe, but rather in the photodetector, the dynamic range could hypothetically be shifted, if necessary, by modifying the sensitivity of the photodetector.

The large (up to $\pm 13\%$) signal variance in measurements obtained over several days renders the system less applicable for monitoring the long-term stability of UHDR linacs. This variance does not demonstrate trends over time or with accumulated dose and is therefore unlikely to be a direct cause of radiation-induced damage to the optical components. Because the temperature of the detector is stabilized before use, it is also unlikely that temperature fluctuations contributed to this variance. The signal variance within each day was low, within $\pm 2\%$, and no drift or trend was apparent. Although no conclusive explanation is apparent for the observed large variance across days, the data indicate that a 'known dose' calibration of the probe is appropriate for each new day of use, and that a subsequent variation within each day of less than $\pm 2\%$ can be expected. The low variance of $\pm 0.2\%$ across immediately subsequent measurements within each triplicate suggests that the relatively higher daily variance of less than $\pm 2\%$, across which the detector was moved and repositioned, may be attributable to positional differences in the physical setup of the detector under the beam.

The data acquired at UHDRs while changing beam parameters ($DR_p = 3.8e3-1.8e6$ Gy/s, $\overline{DR} = 1.8-1,341$ Gy/s, $D_p = 5e-3-7.68$ Gy, PRF = 5-120 Hz, PW = 0.5-4 µs) indicate that these parameters, at least within the tested ranges, seem to not affect the system's dosimetric performance. However, nonlinearity was observed when D_p was increased by increasing DR_p via decreasing the SSD. Similar effects have been seen with other systems(21) and were attributed to the varying amounts of fiber exposed to the radiation field as the SSD was changed, thereby producing varying amounts of contaminating Cherenkov/fluorescence signals. However, we observed that this trend persisted even after recalibration of the system and retaking the data with a collimated field so that the amount of fiber exposed at each SSD was equivalent. Thus, this effect is likely not caused by varying amount of fiber

being exposed, but rather is more likely to be caused by differential effects within the photodetector or in the signal processing with increasing DR_p which needs to be investigated further.

The system's dosimetric information on a pulse-by-pulse basis showed excellent agreement with the BCTs, with the notable exception of 'split pulses', whereby the signal from one pulse was split between two adjacent IWs. This phenomenon is similar to the 'double peaks' reported by Poirier et al., which were understood to occur when the photodetector readout coincided with the delivery of a pulse, leaving part of the pulse on the adjacent integration windows (19). The multi-channel construction and readout of the photodetector renders it partially blind to the pulse when this happens, and thus loses ~10% of the pulse's signal. The automatic processing software of the system was therefore modified to correct for 'double pulses' such that now no signal is lost; but 'split pulses' do occur, in which a small fraction (<5%) of a pulse's signal is recorded in the following integration window. Thus, the resultant relative split does not necessarily reflect the amount of the pulse recorded in either integration window. Split pulses do not affect the total dose reading of a pulsed beam measurement but only affect the peak heights of the individual pulses. Because no signal is lost, the effect can be corrected for as follows: the signal from each pulse is increased by the signal of the immediately following sample, and that sample's signal is decreased by the same amount. Correcting for the split pulse phenomenon for accurate measurement of D_p in FLASH-RT applications is crucial owing to the potential dependence of the FLASH effect on D_n (36,37), as well as the need to meet established recommendations on reporting UHDR beam parameters (4,5).

Because the vendor recommends a sampling frequency of $f_s > 2 * PRF$, there is a mismatch between the delivery and sampling frequencies, leading to inconsistencies in the number of integration windows with and without delivered pulses. For example, for a PRF = 30 Hz delivery measured at $f_s = 70$ Hz, every $\sim 3^{rd}$ pulse will be followed by 2 adjacent integration windows during which no pulse arrives. This leads to an apparent periodic offset in the temporal spacing between pulses that is caused by the discrete nature of the measurement. On average, over multiple pulses, the measured PRF does indeed match the delivered PRF. The maximum PRF the system could differentiate pulses from is limited to <500 Hz by the lowest IW (1 ms); in this work, the system was tested up to 120 Hz, because that is the maximum PRF of the FLASH Mobetron (24,25). For the pulse-by-pulse measurements of 300 pulses, a relatively low D_p of 0.1 Gy was chosen to avoid delivering very large doses to the probe during a single measurement.

As opposed to matching the sample frequency to twice the PRF, a fixed IW of 4.1 ms (f_s =244 Hz) was set for all UHDR measurements. This was done to reflect the aforementioned use of a slightly higher sampling frequency than the Nyquist frequency and to reflect the higher variance in the delivery PRF of the FLASH Mobetron at its maximum output.

This study was limited in part by the output limitations of the FLASH Mobetron. The highest PRF tested was 120 Hz, whereas the scintillation system could theoretically measure a beam PRF of 500 Hz without aliasing effects. The tested D_p and DR_p were limited to 7.68

Gy and 1.8e6 Gy/s, respectively, which safely encompasses the parameter space relevant for clinical electron FLASH administration (33-35). Measuring the dependency of the system on DR_p and PW as D_p was held constant was limited by the slight (up to 3%) variance in the D_p over the tested ranges, and by having only 2 data points (2 PW values) for which a D_p of 4 Gy could be tested. The observed reduction in signal per unit dose as DR_p was increased should be further investigated over a wider range of DR_p . Finally, we did not test the beam energy dependency of the system, having only studied the system using a 9 MeV electron beam in CDR and UHDR conditions. However, this beam quality is representative of many UHDR-compatible systems (24,27,38-44). Moreover, plastic scintillators are known to be energy independent outside the kV energy range in conventional beams (7,8,14,21); however, this should be confirmed also in the UHDR setting.

Conclusions

We performed a comprehensive investigation of the dosimetric performance of the scintillation system across a wide range of irradiation parameters relevant for the clinical translation of electron FLASH RT. The system was linear with dose at both CDRs and UHDRs and showed no dependence on any beam parameters throughout the tested ranges, apart from a 6% signal decrease when the DR_p was increased via the reduction of SSD and the limits of the dynamic range of the photodetector, which requires that the dose per integration window of the photodetector remain within 0.028-11.56 Gy. At the system's highest time resolution of 1ms, D_p measurements of individual pulses could be properly resolved. After applying a simple post-measurement correction for an effect we call 'split pulses', these time-resolved D_p measurements agreed with the BCTs within $\pm 2\%$. Daily variance of the signal remained lower than $\pm 2\%$, but the up to $\pm 13\%$ variance across several days compels a known-dose calibration before each day of use, and limits the system's potential for long term stability monitoring. This study demonstrates the first-todate scintillator dosimetry system capable of providing online and millisecond-resolved dosimetric measurements over the entire dynamic range of CDRs and UHDRs from typical electron linacs, marking an important advancement in UHDR dosimetry and offering diverse applications for FLASH-RT and related fields.

Acknowledgements:

The authors thank François Therriault-Proulx and Benjamin Côté (MedScint, Quebec City, Canada) for their technical advice while performing this work. We also thank Amy Ninetto of the Research Medical Library at MD Anderson Cancer Center and Christine F. Wogan, MS, ELS, of MD Anderson's Division of Radiation Oncology, for editorial contribution to this article.

Funding:

Research reported in this publication was supported in part by the National Cancer Institute of the National Institutes of Health, under Award Number R01CA266673 and Cancer Center Support (COre) Grant P30CA016672 (to The University of Texas MD Anderson Cancer Center); the University Cancer Foundation via the Institutional Research Grant program at MD Anderson; a grant from MD Anderson's Division of Radiation Oncology; a UTHealth Innovation for Cancer Prevention Research Training Program Predoctoral Fellowship (CPRIT RP210042), and by the Klinikum rechts der Isar of the Technical University of Munich. The content is solely the responsibility of the authors and does not necessarily represent the official views of the National Institutes of Health or the Cancer Prevention and Research Institute of Texas.

Data Sharing:

The raw data supporting the conclusion of this article will be made available by the authors upon reasonable request.

References

- 1. Romano F, Bailat C, Jorge PG, et al. Ultra-high dose rate dosimetry: Challenges and opportunities for flash radiation therapy. Medical physics 2022;49:4912–4932. [PubMed: 35404484]
- 2. Liu K, Holmes S, Hooten B, et al. Evaluation of ion chamber response for applications in electron flash radiotherapy. Medical physics 2023.
- 3. Di Martino F, Barca P, Barone S, et al. Flash radiotherapy with electrons: Issues related to the production, monitoring, and dosimetric characterization of the beam. Frontiers in Physics 2020:8:570697.
- Schüler E, Acharya M, Montay-Gruel P, et al. Ultra-high dose rate electron beams and the flash effect: From preclinical evidence to a new radiotherapy paradigm. Medical physics 2022;49:2082– 2095. [PubMed: 34997969]
- Zou W, Zhang R, Schueler E, et al. Framework for quality assurance of ultra-high dose rate clinical trials investigating flash effects and current technology gaps. International Journal of Radiation Oncology* Biology* Physics 2023.
- Tanderup K, Beddar S, Andersen CE, et al. In vivo dosimetry in brachytherapy. Medical physics 2013;40:070902. [PubMed: 23822403]
- Beddar A, Mackie T, Attix F. Water-equivalent plastic scintillation detectors for high-energy beam dosimetry: I. Physical characteristics and theoretical considerations. Physics in Medicine & Biology 1992;37:1883. [PubMed: 1438554]
- 8. Beddar AS, Mackie TR, Attix FH. Water-equivalent plastic scintillation detectors for high-energy beam dosimetry: Ii. Properties and measurements. Physics in Medicine & Biology 1992;37:1901. [PubMed: 1438555]
- Clift M, Sutton R, Webb D. Dealing with cerenkov radiation generated in organic scintillator dosimeters by bremsstrahlung beams. Physics in Medicine & Biology 2000;45:1165. [PubMed: 10843098]
- 10. Thrower S, Prajapati S, Holmes S, et al. Characterization of the plastic scintillator detector system exradin w2 in a high dose rate flattening-filter-free photon beam. Sensors 2022;22:6785. [PubMed: 36146135]
- 11. Clift M, Johnston P, Webb D. A temporal method of avoiding the cerenkov radiation generated in organic scintillator dosimeters by pulsed mega-voltage electron and photon beams. Physics in Medicine & Biology 2002;47:1421. [PubMed: 12030564]
- 12. Beddar A, Mackie T, Attix F. Cerenkov light generated in optical fibres and other light pipes irradiated by electron beams. Physics in Medicine & Biology 1992;37:925.
- Torrisi L. Plastic scintillator investigations for relative dosimetry in proton-therapy. Nuclear Instruments and Methods in Physics Research Section B: Beam Interactions with Materials and Atoms 2000;170:523–530.
- Archambault L, Polf JC, Beaulieu L, et al. Characterizing the response of miniature scintillation detectors when irradiated with proton beams. Physics in Medicine & Biology 2008;53:1865.
 [PubMed: 18364543]
- 15. Mascia AE, Daugherty EC, Zhang Y, et al. Proton flash radiotherapy for the treatment of symptomatic bone metastases: The fast-01 nonrandomized trial. JAMA oncology 2023;9:62–69. [PubMed: 36273324]
- 16. Lee E, Lourenço AM, Speth J, et al. Ultrahigh dose rate pencil beam scanning proton dosimetry using ion chambers and a calorimeter in support of first in-human flash clinical trial. Medical Physics 2022;49:6171–6182. [PubMed: 35780318]

17. Cecchi DD, Therriault-Proulx F, Lambert-Girard S, et al. Characterization of an x-ray tube-based ultrahigh dose-rate system for in vitro irradiations. Medical Physics 2021;48:7399–7409. [PubMed: 34528283]

- 18. Favaudon V, Lentz J-M, Heinrich S, et al. Time-resolved dosimetry of pulsed electron beams in very high dose-rate, flash irradiation for radiotherapy preclinical studies. Nuclear Instruments and Methods in Physics Research Section A: Accelerators, Spectrometers, Detectors and Associated Equipment 2019;944:162537.
- Poirier Y, Xu J, Mossahebi S, et al. Characterization and practical applications of a novel plastic scintillator for online dosimetry for an ultrahigh dose rate (flash). Medical Physics 2022;49:4682– 4692. [PubMed: 35462420]
- 20. Ashraf MR, Rahman M, Cao X, et al. Individual pulse monitoring and dose control system for pre-clinical implementation of flash-rt. Physics in Medicine & Biology 2022;67:095003.
- 21. Liu K, Holmes S, Schüler E, et al. A comprehensive investigation of the performance of the exradin w2 scintillator system for applications in electron flash radiotherapy. Medical physics 2023.
- 22. Therriault-Proulx F, Archambault L, Beaulieu L, et al. Development of a novel multi-point plastic scintillation detector with a single optical transmission line for radiation dose measurement. Physics in Medicine & Biology 2012;57:7147. [PubMed: 23060069]
- Almond PR, Biggs PJ, Coursey BM, et al. Aapm's tg-51 protocol for clinical reference dosimetry of high-energy photon and electron beams. Medical physics 1999;26:1847–1870. [PubMed: 10505874]
- 24. Moeckli R, Gonçalves Jorge P, Grilj V, et al. Commissioning of an ultra-high dose rate pulsed electron beam medical linac for flash rt preclinical animal experiments and future clinical human protocols. Medical physics 2021;48:3134–3142. [PubMed: 33866565]
- 25. Palmiero A, Liu K, Colnot J, et al. On the acceptance, commissioning, and quality assurance of electron flash units. arXiv preprint arXiv:240515146 2024.
- 26. Liu K, Jorge PG, Tailor R, et al. Comprehensive evaluation and new recommendations in the use of gafchromic ebt3 film. Medical physics 2023.
- 27. Liu K, Palmiero A, Chopra N, et al. Dual beam-current transformer design for monitoring and reporting of electron ultra-high dose rate (flash) beam parameters. Journal of applied clinical medical physics 2023;24:e13891. [PubMed: 36601691]
- 28. Goncalves Jorge P, Grilj V, Bourhis J, et al. Validation of an ultrahigh dose rate pulsed electron beam monitoring system using a current transformer for flash preclinical studies. Medical Physics 2022;49:1831–1838. [PubMed: 35066878]
- 29. Timakova E, Zavgorodni SF, Bazalova-Carter M. Characterization of a 0.8 mm3 medscint plastic scintillator detector system for small field dosimetry. Physics in Medicine and Biology 2023.
- 30. Jean E, Therriault-Proulx F, Beaulieu L. Comparative optic and dosimetric characterization of the hyperscint scintillation dosimetry research platform for multipoint applications. Physics in Medicine & Biology 2021;66:085009.
- 31. Uijtewaal P, Côté B, Foppen T, et al. Performance of the hyperscint scintillation dosimetry research platform for the 1.5 t mr-linac. Phys Med Biol 2023;68.
- 32. Schoepper I, Dieterich S, Trestrail EA, et al. Pre-clinical and clinical evaluation of the hyperscint plastic scintillation dosimetry research platform for in vivo dosimetry during radiotherapy. J Appl Clin Med Phys 2022;23:e13551. [PubMed: 35188331]
- 33. Vozenin M-C, Bourhis J, Durante M. Towards clinical translation of flash radiotherapy. Nature Reviews Clinical Oncology 2022;19:791–803.
- 34. Kinj R, Gaide O, Jeanneret-Sozzi W, et al. Randomized phase ii selection trial of flash and conventional radiotherapy for patients with localized cutaneous squamous cell carcinoma or basal cell carcinoma: A study protocol. Clinical and Translational Radiation Oncology 2024:100743. [PubMed: 38362466]
- 35. Loo BW Jr, Verginadis II, Sørensen BS, et al. Navigating the critical translational questions for implementing flash in the clinic. Seminars in Radiation Oncology. Elsevier. 2024. pp. 351–364.
- 36. Liu K, Waldrop T, Aguilar E, et al. Redefining flash rt: The impact of mean dose rate and dose per pulse in the gastrointestinal tract. bioRxiv 2024:2024.04. 19.590158.

37. Ruan J-L, Lee C, Wouters S, et al. Irradiation at ultra-high (flash) dose rates reduces acute normal tissue toxicity in the mouse gastrointestinal system. International Journal of Radiation Oncology* Biology* Physics 2021;111:1250–1261. [PubMed: 34400268]

- 38. Schüler E, Trovati S, King G, et al. Experimental platform for ultra-high dose rate flash irradiation of small animals using a clinical linear accelerator. International Journal of Radiation Oncology* Biology* Physics 2017;97:195–203. [PubMed: 27816362]
- 39. Kim MM, Darafsheh A, Schuemann J, et al. Development of ultra-high dose-rate (flash) particle therapy. IEEE transactions on radiation and plasma medical sciences 2021;6:252–262. [PubMed: 36092270]
- 40. Lempart M, Blad B, Adrian G, et al. Modifying a clinical linear accelerator for delivery of ultrahigh dose rate irradiation. Radiotherapy and Oncology 2019;139:40–45. [PubMed: 30755324]
- 41. Oesterle R, Gonçalves Jorge P, Grilj V, et al. Implementation and validation of a beam-current transformer on a medical pulsed electron beam linac for flash-rt beam monitoring. Journal of Applied Clinical Medical Physics 2021;22:165–171.
- 42. Jaccard M, Durán MT, Petersson K, et al. High dose-per-pulse electron beam dosimetry: Commissioning of the oriatron ert6 prototype linear accelerator for preclinical use. Medical physics 2018;45:863–874. [PubMed: 29206287]
- FLASHKNiFE THERYQ. https://www.flashknife-project.com/project/. Accessed September 19, 2024
- 44. ElectronFlash SIT-Sordina IORT Technologies. https://www.soiort.com/flash-rt-technology/. Accessed September 19, 2024.

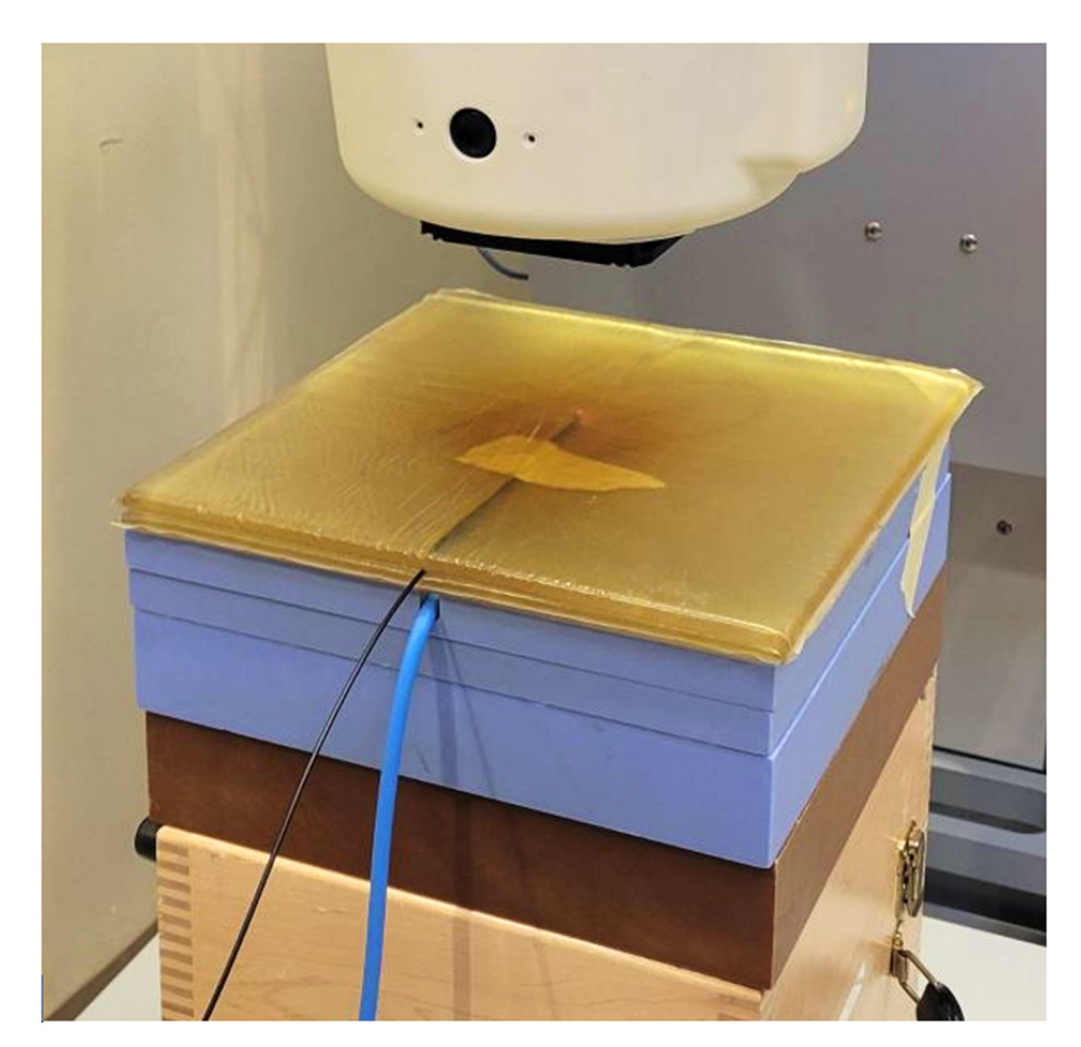


Figure 1.

Measurement setup of the scintillator probe under the Mobetron beamline. Tape was used to secure the probe in place between the two sheets of semi-transparent bolus material. The white treatment head of the Mobetron is visible at the top of the image. Also visible is the blue cable from the ionization chamber (included only during conventional dose rate measurements), which is embedded in the 2 cm of solid water directly below the bolus material.

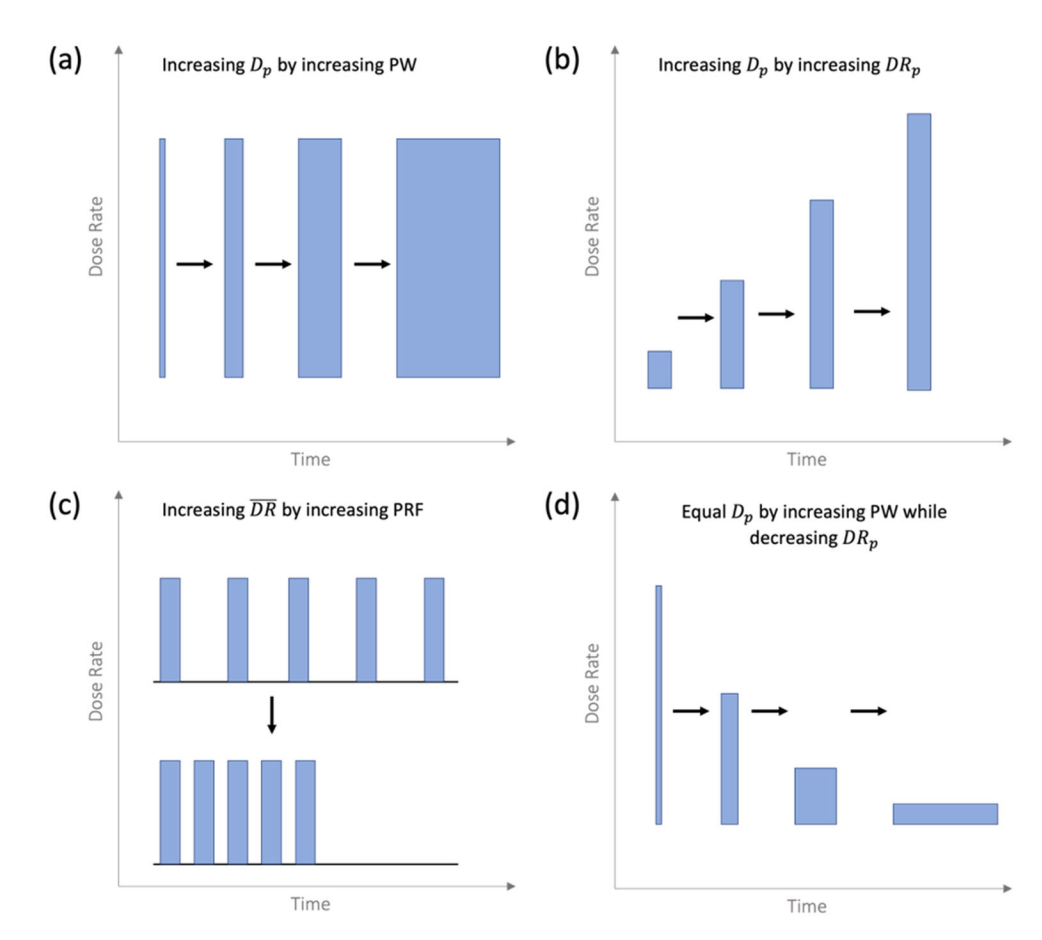


Figure 2. Schematic of the various pulsed beam parameters and how they were modulated in the evaluation of the scintillator system. The black arrows indicate what was being compared in each experiment type: (a) the effect of increasing the dose per pulse (D_p) by increasing the pulse width (PW), (b) the effect of increasing D_p by increasing the pulse dose rate DR_p , (c) the effect of increasing the mean dose rate \overline{DR} by increasing the pulse repetition frequency (PRF), and (d) the effect of maintaining a constant D_p while simultaneously increasing PW and decreasing DR_p .

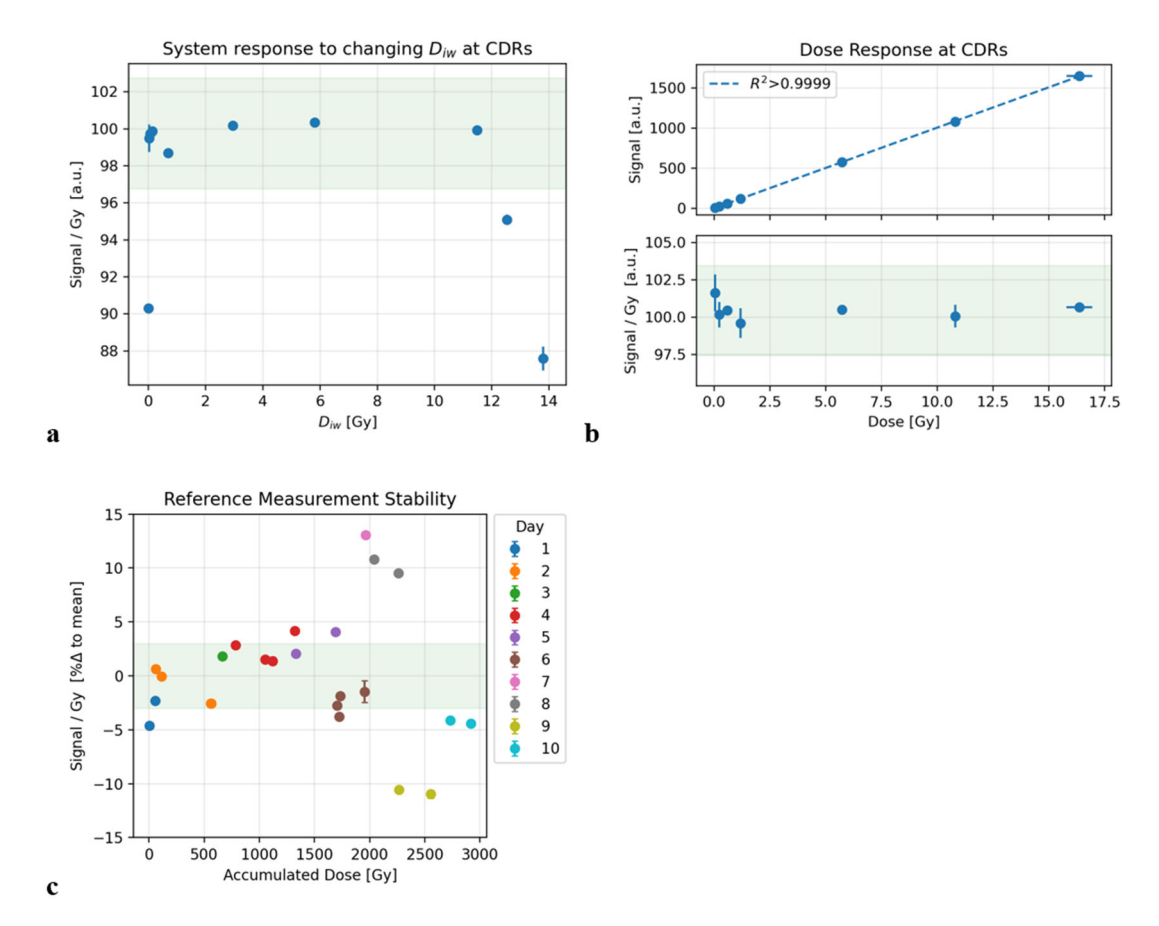
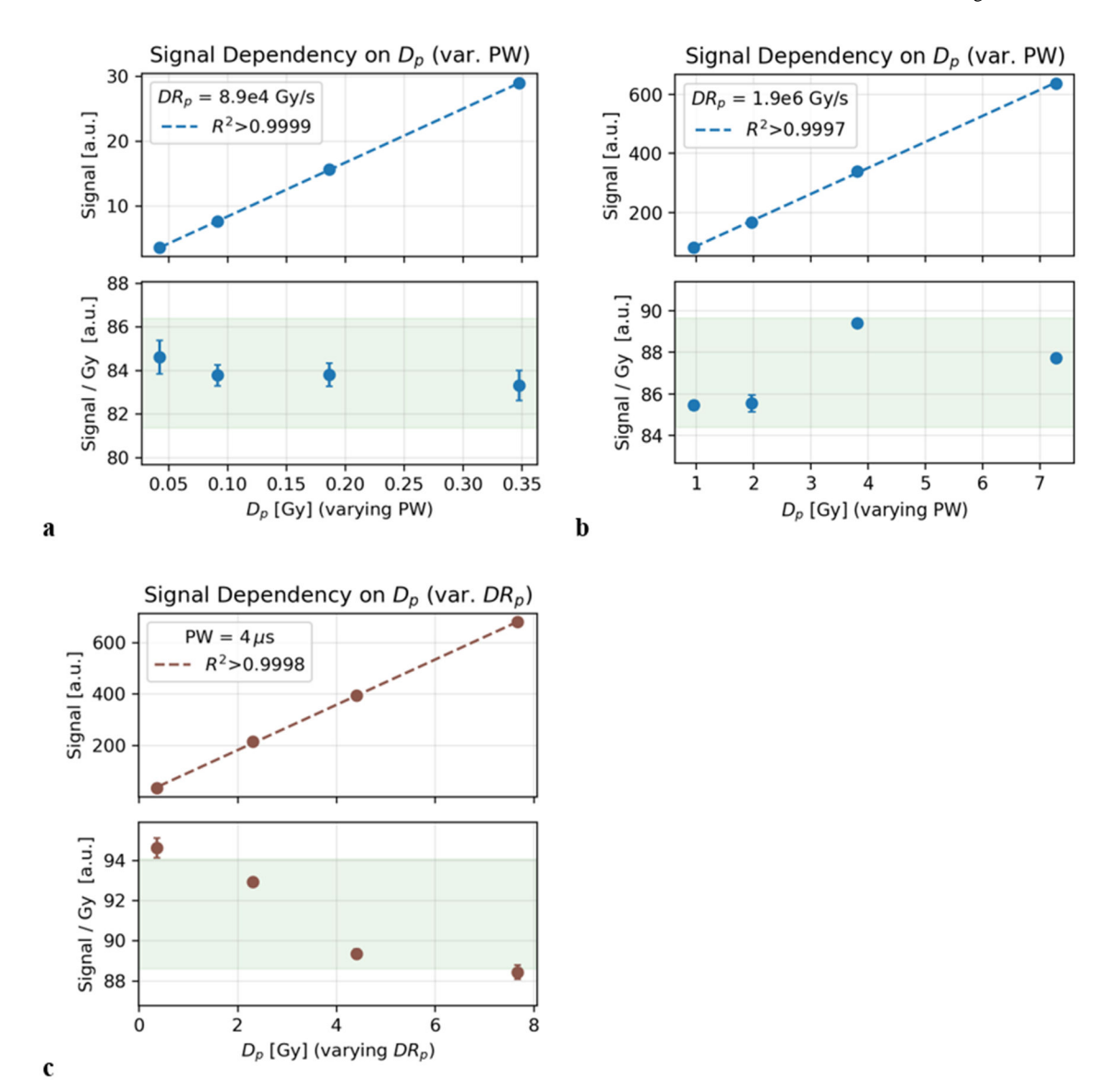
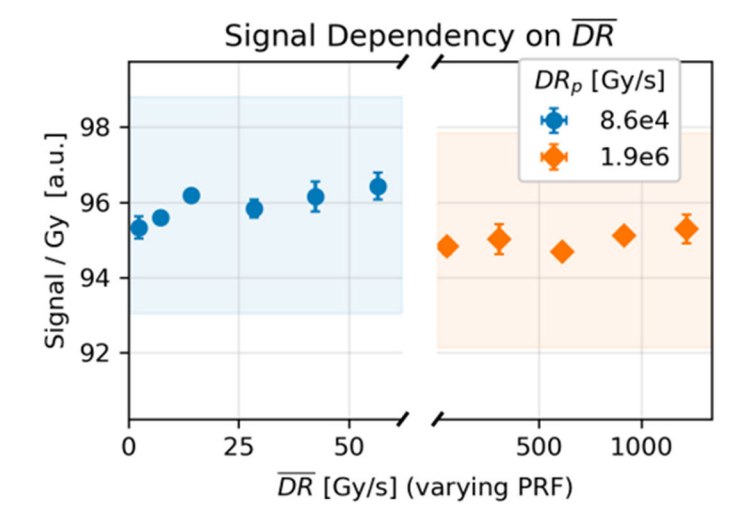


Figure 3. System dose response and stability at CDRs. (a) Signal per unit dose over a wide range of the dose per integration window (D_{iw}) from 0.007–13.94 Gy (the specific parameters are shown in Table 1, **experiment I**). (b) Dose response (top) and signal per unit dose (bottom) at CDRs, wherein D_{iw} was kept between 0.05 and 0.14 Gy (Table 1 **experiment II**). (c) Dose-normalized signal change, reported as a percent change relative to the mean, in the reference setup over 10 non-consecutive days of measurements and ~3 kGy of accumulated dose (Table 1 **experiment III**). Each day's measurements are indicated in a unique color. The green shaded region indicates a $\pm 3\%$ variance from the mean.



Dose response as D_p was increased by increasing PW at constant values of DR_p of either (a) 8.9e4 Gy/s or (b) 1.9e6 Gy/s (Table 1 **experiment IV**). (c) The signal increased linearly with D_p as the DR_p was increased at a constant PW (Table 1 **experiment V**). The signal per unit dose decreased with increasing DR_p . The green shaded region indicates a $\pm 3\%$ variance from the mean.



a

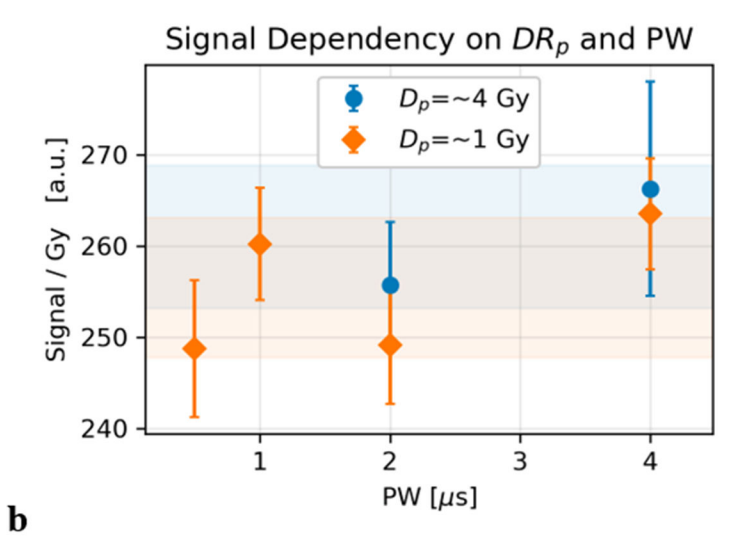


Figure 5.(a) Dose-normalized signal change as \overline{DR} was varied by changing the PRF at two values of DR_p (Table 1 **experiment VII**). (b) PW was varied alongside DR_p to maintain equivalent values of D_p at 4 ± 0.12 Gy and 1 ± 0.02 Gy (Table 1 **experiment VIII**). In both (a) and (b), a $\pm 3\%$ variance from the mean for each dataset is indicated by the shaded regions, with colors corresponding to the DR_p or D_p values shown.

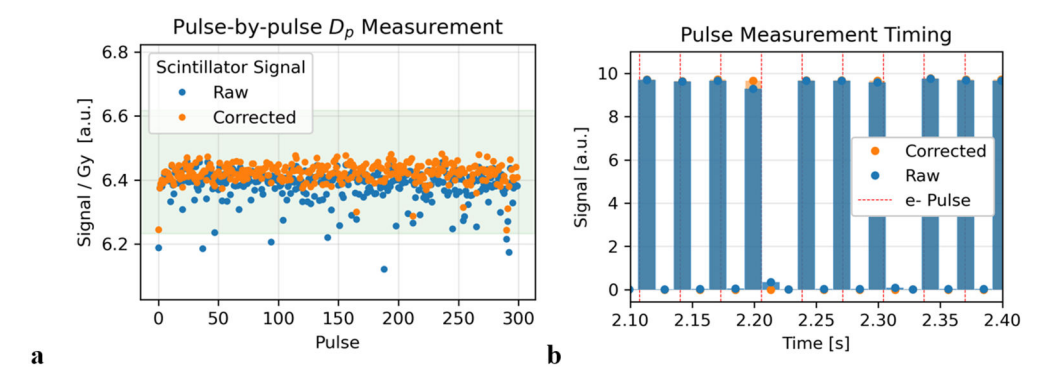


Figure 6. (a) The dose-normalized scintillator signal, raw and corrected, across all 300 pulses of the delivery. The correction was applied to the raw signal to correct for the occurrence of 'split pulses'. (b) A ten-pulse excerpt from a 300-pulse, PRF =30 Hz delivery measured at sampling frequency (f_s) of 70 Hz demonstrating the effect of the correction. The hypothesized timing of the electron pulses delivered at 30 Hz that could have caused the observed split pulses is overlaid onto the measured signal. The green shaded region indicates a $\pm 3\%$ variance from the mean.

Author Manuscript

Author Manuscript

Table 1.

Parameters used in experiments performed in this work.

Experiment	Experiment SSD, cm	PRF, Hz	$F, { m Hz} PW, { m \mu s} N_{ m ho}$		$D, Gy D_p, Gy$	$D_{ ho}$, Gy	$DR_{ ho}$, Gy/s	\overline{DR} , Gy/s	$IW, \mathrm{s} D_{iw}$	D_{iw}
I	35.8	30	1.2	476–2788	476–2788 2.38 – 13.94 5e-3	5e-3	3.8e3	0.14	0.05-180	0.05–180 7e-3–13.9
п	35.8	30	1.2	10-3440	0.05–17.20 5e-3	5e-3	3.8e3	0.14	1	0.05-0.14
H	35.8	30	1.2	484 ± 8	2.42 ± 0.04	5e-3	3.8e3	0.14	1	0.14
IV	25.8; 111.2	30	0.5-4	æ	0.12–1.05 2.85–21.8	0.04-0.4 0.95-7.3 8.6e4; 1.9e6	8.6e4; 1.9e6	1.80–15.8 42.8–328	4.1e-3	0.04–0.35 0.95–7.28
>	25.8-111.2	30	4	3	1.08-23.1	0.36-7.7	8.6e4-1.9e6	16.2–347	4.1e-3	0.36-7.71
IA	25.8; 111.2	5-120	4	3	0.96; 20.8	0.32; 6.9	8e4-1.7e6	2.4–57.6; 51.8–1244	4.1e-3	0.96; 20.7
М	25.8–68.8; 25.8–33.8 30	30	0.5-4; 2-4	3	3.00; 12.03	1.00; 4.01	2.5e5–2e6; 1e6–2e6 45; 181	45; 181	4.1e-3	1.00; 4.01
VIII	111.2	30	1	300	30	0.1	0.1e6	3.01	4.1e-3	0.1

Experiments:

I Dependence on D_{lw} at conventional dose rates

II Dependence on D at conventional dose rates

III Stability at conventional dose rates

IV Dependence on D_p by increasing PW

V Dependence on $D_{\scriptscriptstyle p}$ by increasing $DR_{\scriptscriptstyle p}$

VI Dependence on \overline{DR} by increasing PRF

VII Dependence on PW and $DR_{
ho}$ at constant $D_{
ho}$

VIII Pulse-by-pulse measurement of $D_{
ho}$

Abbreviations: SSD, source to surface distance; PRF, pulse repetition frequency; PW, pulse width; N_p , number of pulses; D, total dose; D_p , dose per pulse; DR_p pulse dose rate; \overline{DR} , mean dose rate; IW, detector integration window; D_{lw} , dose per integration window.